Dev Genes Evol (2003) 213:612–624
DOI 10.1007/s00427-003-0365-1

ORIGINAL ARTICLE

Jeffrey S. Kauffman · Rudolf A. Raff

Patterning mechanisms in the evolution of derived developmental life histories: the role of Wnt signaling in axis formation of the direct-developing sea urchin *Heliocidaris erythrogramma*

Received: 28 July 2003 / Accepted: 17 October 2003 / Published online: 15 November 2003

Abstract A number of echinoderm species have replaced indirect development with highly modified direct-developmental modes, and provide models for the study of the evolution of early embryonic development. These divergent early ontogenies may differ significantly in life history, oogenesis, cleavage pattern, cell lineage, and timing of cell fate specification compared with those of indirect-developing species. No direct-developing echinoderm species has been studied at the level of molecular specification of embryonic axes. Here we report the first functional analysis of Wnt pathway components in *Heliocidaris erythrogramma*, a direct-developing sea urchin. We show by misexpression and dominant negative knockout construct expression that *Wnt8* and *TCF* are functionally conserved in the generation of the primary (animal/vegetal) axis in two independently evolved direct-developing sea urchins. Thus, Wnt pathway signaling is an overall deeply conserved mechanism for axis formation that transcends radical changes to early developmental ontogenies. However, the timing of expression and linkages between *Wnt8*, *TCF*, and components of the PMC-specification pathway have changed. These changes correlate with the transition from an indirect- to a direct-developing larval life history.

Keywords Wnt signaling · Sea urchin · Axis specification · Evolution of development

Edited by D. Tautz

J. S. Kauffman · R. A. Raff (✉)
Department of Biology,
Indiana University,
Myers Hall 102, Bloomington, IN 47405, USA
e-mail: rraff@bio.indiana.edu
Tel.: +1-812-8552791
Fax: +1-812-8556082

Introduction

The genus *Heliocidaris* contains two sister species, approximately 4 million years diverged (Zigler et al. 2003). *H. tuberculata* undergoes a process of indirect development essentially identical to that seen in most other sea urchins (Okazaki 1975; Davidson et al. 1998). *H. erythrogramma* exhibits a radically different mode of larval development; it forms a non-feeding larva which precociously develops a rudiment immediately following gastrulation (Williams and Anderson 1975; Raff 1996). Some changes in the derived developmental program of *H. erythrogramma* reflect losses of larval feeding features (Raff et al. 1999), whereas others are gains of novel features (Henry and Raff 1990; Wray and Raff 1990; Byrne et al. 1999; Villinski et al. 2002). These include a new terminal phase of oogenesis, a much larger egg, a change in egg protein and lipid composition, a new mode of cleavage, and a novel cell lineage. The animal/vegetal (A/V) axis remains maternally determined, and the left-right and dorso-ventral axes have become maternally determined as well.

The molecular nature of determination of the A/V axis in sea urchins is not fully understood, although maternal specification of the A/V axis is conserved among echinoderm classes (Goldstein and Freeman 1997). However, timing and patterning of initial cell types along the A/V axis have evolved radically during the evolution of direct-developing sea urchin species. We studied the development of the A/V axis of *H. erythrogramma* to provide a foundation for studies of the evolution of this and other more divergent embryonic axes. We asked whether the molecular components of A/V axis expression in direct-developing sea urchins were conserved relative to indirect-developing species.

Among indirect-developing sea urchins the four most vegetal blastomeres are the products of an asymmetric sub-equatoral fourth cleavage event, which produces four micromeres (Fig. 1B). No micromeres are formed in *H. erythrogramma* (Fig. 1A), although cell fates derived

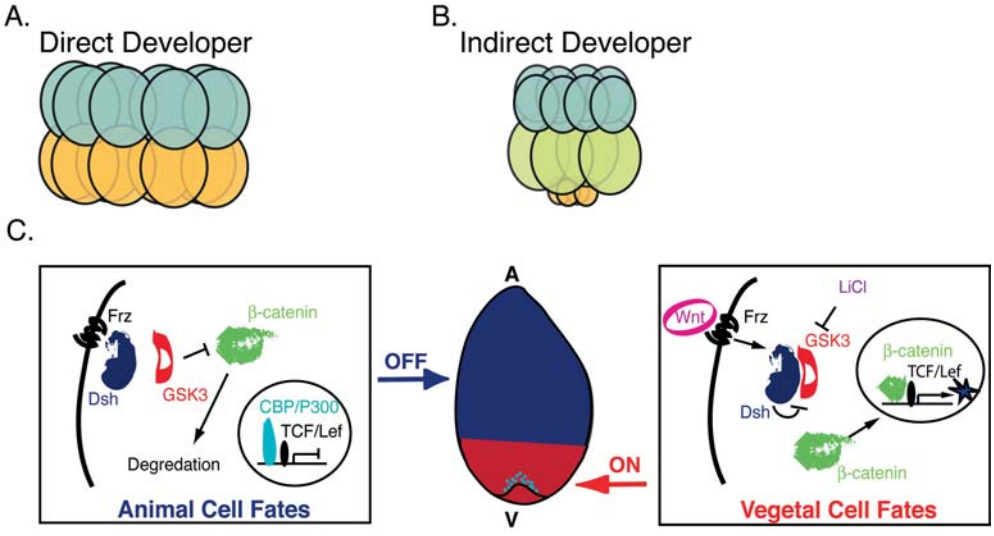

Fig. 1 **A** A schematic of a 16-cell-stage *Heliocidaris erythrogramma* embryo. There are two tiers of blastomeres and cleavage is equal. **B** A schematic of a typical 16-cell-stage indirect-developing sea urchin embryo. The fourth cleavage, while equal in the animal pole blastomeres, is unequal among the vegetal blastomeres. **C** A schematic of the canonical Wnt signaling pathway. The canonical Wnt signaling pathway is inactive in animal pole cells resulting in ectodermal cell fates (*red*). Active signaling of the Wnt pathway in vegetal cells results in the specification of vegetal-plate-derived tissues, mesenchyme, and mesendodermal cell fates (indicated in *blue*). In the absence of a Wnt ligand, GSK3 constitutively phosphorylates *β*-catenin marking it for ubiquitination. In the presence of a Wnt ligand, or Li, GSK3 is inactivated thereby permitting *β*-catenin levels to increase and free *β*-catenin then translocates to the nucleus, and interacts with TCF/Lef to activate transcription of Wnt responsive genes (Cadigan and Nusse 1997; Emily-Fenouil et al. 1998; Vonica et al. 2000; Huang et al. 2000; Sharpe et al. 2001)

from micromeres in indirect-developers (skeletogenic cells and coelomic precursors) arise later in *H. erythrogramma* development from vegetal pole cells (Wray and Raff 1989, 1990). The micromeres of the indirect-developing sea urchin embryo constitute an organizing center (Wikramanayake and Klein 1997). Embryological experiments show that transplantation of large micromeres to ectopic sites can induce a second axis to form (Ransick and Davidson 1993, 1995).

The absence of morphological differentiation at the 16-cell stage in the *H. erythrogramma* embryo poses the question: are there a subset of cells in the 16-cell-stage embryo that act as a vegetal organizing center, or has there been a heterochronic shift in timing of organizer function in *H. erythrogramma*? Embryological and fate mapping data indicate that many patterning events in *H. erythrogramma* are heterochronically shifted relative to indirect-developing sea urchins. Specification of primary mesenchyme cell (PMC) fates are not segregated until after the 64-cell stage (Wray and Raff 1990; and possibly not until after the 128-cell stage) in *H. erythrogramma.* However, PMCs are specified at the 32-cell stage in indirect-developers (Cameron et al. 1987). However, secondary mesenchyme cell (SMC) and mesendoderm cell fates segregate at roughly the same time in both developmental modes, and vegetal ectoderm segregates earlier in the direct-developing lineage (Henry and Raff 1990; Wray and Raff 1990).

Signaling through the canonical Wnt pathway (Fig. 1C) begins at the 16-cell stage in the micromeres of indirect-developing sea urchins and is the primary effector of vegetal axis specification (Logan et al. 1999; Huang et al. 2000; Vonica et al. 2000; Brandhorst and Klein 2002). Recent work with *Wnt8* in the indirect-developing sea urchin *Strongylocentrotus purpuratus* has revealed its involvement in A/V axis specification, specifically in SMC and mesendoderm patterning (reviewed in Brandhorst and Klein 2002). The absence of an unequal fourth cleavage in *H. erythrogramma* and the delay in mesenchyme cell specification are both significant, and raise the question of how Wnt signaling, and specifically *TCF*, *Wnt8* and *β-catenin*, pattern the vegetal axis of the direct-developing sea urchin *H. erythrogramma*.

Data from two sea urchin species indicate a conserved role for the canonical Wnt pathway in establishment of the urchin A/V axis (Brandhorst and Klein 2002; Davidson et al. 2002; Angerer and Angerer 2003). Both species are indirect-developing sea urchins, which exhibit the conserved, ancestral mode of indirect development via a pluteus larva. Nearly 20% of sea urchins do not exhibit indirect development (Emlet et al. 1987; Raff 1987). We asked if the role of the Wnt pathway is functionally conserved in the divergent early ontogeny of a direct-developing sea urchin in which the embryonic and larval ontogenies are highly modified.

Our goal was to determine if vegetal specification in early embryogenesis via the canonical Wnt pathway is conserved in the direct-developing sea urchin *H. erythrogramma* and to explore the functional roles of *Wnt8*, *TCF*, and *β-catenin* in axis patterning. This is the first functional study of a signaling pathway in a direct-

developing sea urchin. We had three objectives. The first was to determine if *H. erythrogramma* is amenable to functional studies using RNA injections for transient expression of a range of gene products, from ligands to transcription factors. Second, we wished to test if the Wnt pathway is conserved in its role of patterning the A/V axis of an evolutionarily modified direct-developing sea urchin larva. Finally, we evaluated the hypothesis that components of functionally conserved signaling pathways can evolve over relatively short evolutionary periods of time.

We injected a number of Wnt pathway components, and have examined the functional linkage between *TCF* and *Wnt8* via mRNA misexpression and knockout, as well as lithium treatment. We demonstrate that the general mechanism of Wnt specification of the vegetal axis is an evolutionarily conserved echinoid trait through functional studies in *H. erythrogramma* and *Holopneustes purpurescens*, another independently derived direct-developing sea urchin species.

Our data suggest that heterochronic shifts in the timing of *TCF* signaling have potentially altered the competence of some blastomeres to form pluteus structures in the direct-developing species. We propose that the Wnt pathway gene products generate similar functional phenotypes in both indirect and direct-developing sea urchins. However, changes in the timing of gene expression and linkages between genes may have altered the timing of cell fate specification, and this may be considered evidence that the genetic pathways have begun to diverge in *H. erythrogramma* from the state observed in indirect-developing species.

Materials and methods

Cloning and expression constructs

HeWnt8 was cloned from an *Heliocidaris erythrogramma* gastrula-stage cDNA library following Ferkowicz et al. (1998). The *EN-SpTCF* and *VP16xTCF3* DNAs were gifts of J. Venuti. Full length *HeWnt8* was subcloned into pCS2+ expression vector. Dominant negative *SpWnt8* (*DN-SpWnt8*) was a gift of A. Wikramanayake.

Microinjection of RNAs

Capped RNAs were synthesized from linearized DNA templates using the mMessage mMachine kit (Ambion). RNAs were extracted twice with phenol-chloroform and quantitated by spectrophotometry. RNA integrity was confirmed by gel electrophoresis. RNAs were suspended in 10 mM Tris pH 7.6 at 2 μg/μl and this solution was used as a stock solution for injections. Injection buffers final concentration was 0.2 M KCl, 20% glycerol, 100 μg/μl dextran-conjugated Texas red (Molecular Probes). Microinjection volumes were 70–100 pl using a Picospritzer II with continuous pressure flow. Unfertilized eggs were injected and then allowed to rest for 15 min before fertilization. Embryos were cultured in MPFSW at a concentration of no more than 1 embryo per ml, with daily water changes. Embryos were checked for Texas-red fluorescence before fixation, and then were fixed in 2% paraformaldehyde.

Imaging

Embryos were imaged on a Zeiss Axiophot microscope. For pigment cell counts, live embryos were immobilized on slides and pigment cells counted on the ventral half of the embryo. Pigment cell statistics were calculated using Statview 5.0, and significance was determined using a paired *t*-test. Images of live embryos were taken with 64T Kodachrome film. Slide images were scanned and imported in TIFF format to Photoshop 7.0 (Adobe). Fixed samples and in situ hybridizations were imaged with a SpotRT digital camera and files were then imported to Photoshop 7.0 for analysis.

Alkaline phosphatase staining

Fixed embryos were rehydrated, washed with 1× PBS 3 times, and finally washed 3 times in staining buffer (same as staining buffer used for in situ hybridization staining reactions except levamisole concentration is reduced to 0.3 mM.) Embryos were then transferred to staining buffer with NBT/BCIP and allowed to stain in the dark.

In situ hybridization

In situ hybridizations were carried out following Sly et al. (2002). However, embryos were treated with 0.5% H_2O_2 for 10 min prior to proteinase K digestion, and immediately after proteinase K digestion were washed in 2 mg/ml glycine. Following the color development reactions embryos were dehydrated, and embedded in wax for sectioning. Embryos were sectioned in 9-μm thicknesses.

Immuno-histochemistry

Paraformaldehyde-fixed embryos were washed 4 times in PBT then blocked for 1 h at room temperature in 7% normal goat serum, 4% sheep serum in PBS. The antibody B2C2, a monoclonal antibody against the protein MSP130 (Parks et al. 1988), was used to mark PMCs. Antibody was applied at 1:100 in PBS with 3% normal goat serum, and 1% sheep serum for 1 h at room temperature. Embryos were washed 4 timers for 10 min each in PBT, then incubated in anti mouse-AP secondary antibody for 1 h at room temperature. Embryos were then washed 4 times in PBT and stained for the alkaline phosphatase-conjugated antibody.

RT-PCR

RT-PCR was preformed on 100 ng total RNA per reaction for all experiments. Total RNA samples for developmental timing of *HeWnt8* expression were collected as described (Kauffman et al. 2003). Embryos injected with *EN-SpTCF* mRNA were collected at the mid-gastrula stage, and RNA was extracted from 20 embryos using Trizol with glycogen (Gibco BRL) as a nucleic acid carrier. RNA from control embryos from the same female was also extracted, as well as RNA from uninjected eggs. RNA samples were treated with DNaseI (2 U/μg) for 15 min at 37°C, and inactivated by incubation at 65°C for 15 min. RT-PCR was carried out using the Qiagen One Step RT-PCR mix. *HeWnt8* RT-PCR primer sequences were HeW85 5′-cgttggggacgagatcaagc-3′, and HeW83 5′-cgcacttcacctgacagcac-3′, and *EF1α* RT-PCR primer sequences were Ef15 5′-agattccggcaagtcaaccac-3′, and Ef13 5′-tggccatccttggatatacca-3′. RT-PCR reactions were carried out at 50°C for 30 min. PCR reactions used an annealing temperature of 54°C, for Fig. 3A, and PCR reactions used 25 cycles; for Fig. 3B, 28 cycles of PCR were used. RT minus and positive control reactions were carried out simultaneously with *HeWnt8*, or *HeEF1α* (control) PCR primers.

Results

Morphological assessment of *H. erythrogramma* development

In *H. erythrogramma* control embryos, gastrulation occurs around 18 h post fertilization (Fig. 2A). The blastula elongates along the animal vegetal axis as gastrulation proceeds. By the late gastrula/early larva stage the left coelom begins to form, and a region of ectoderm on the left quadrant of the embryo thickens and begins to differentiate into vestibular ectoderm (Fig. 2A). At 55 h of development, mid-larva stage, the five tubefeet can be seen just below the left-side larval ectoderm (Fig. 2G, M). A ciliary band forms near the vegetal end of the embryo. Pigment cells are distributed throughout the extra-vestibular ectoderm of the embryo, most heavily at the vegetal pole where they originate. Pigment cells are not found in the ciliary band or vestibular ectoderm. Mid-larva-stage control embryos form an arrayed lattice of mesenchyme cells within the animal pole. The cells of the ectoderm are columnar and the coelomic/mesodermal tissues of the rudiment are well developed (Fig. 2M). Phenotypes of embryos injected with, or treated by, agents that perturb the Wnt pathway are assessed by comparison with these features of control embryos.

The effect of LiCl on *H. erythrogramma* development

LiCl produces a vegetalization phenotype in *H. erythrogramma* similar to the vegetalization observed in indirect-developing sea urchins (Cameron and Davidson 1997; Takata et al. 2002). Strong vegetalization effects are seen with 20 mM LiCl. Control embryos were cultured in either FSW or FSW supplemented with 20 mM NaCl. A few embryos, (approximately 15–20%) exogastrulated during treatment. A similar number exogastrulated in control NaCl-treated cultures.

LiCl treatment results in a significant increase in most vegetal-plate-derived tissues including pigment cells (Table 1; Fig. 2B, H). Pigment cells are secondary mesenchyme cell derivatives. Increased pigment cell number is therefore a measure of secondary mesenchyme production. Treated embryos fail to elongate and maintain the rounded shape of a pre-gastrula embryo. The ectoderm is rough in appearance and sectioning indicates that the normally columnar ectoderm (Fig. 2H, N) forms a mixture of columnar and cuboidal cells. Embryos treated with 20 mM LiCl do not form a ciliary band and vestibular ectoderm does not differentiate. Internally, LiCl-treated embryos appear to be filled with a mass of vegetal-plate-derived tissues (Fig. 2H). LiCl-treated embryos show a reduced blastocoelar space, and the mesenchyme cell lattice is irregularly organized (Fig. 2N).

The role of *TCF* in *H. erythrogramma* development

EN-SpTCF is a dominant negative expression construct generated by fusing *S. purpuratus TCF* to an engrailed repressor domain (J. Venuti, unpublished). Injection of *EN-SpTCF* mRNA into *H. erythrogramma* results in animalization. Injected embryos exhibit a pale ectoderm, with few pigment cells (Figure 2C, I). Pigment cell counts indicate a significant decrease in pigment cell formation in injected mid-larval-stage embryos compared with controls (Table 1). About 50% of embryos form multi-lobate structures (seen in Fig. 2C). The ectodermal walls collapse into the blastocoelar space forming a deeply wrinkled surface. Embryos do not gastrulate after 0.8 μg/μl *EN-SpTCF* injection (not shown). Embryos injected with 0.5 μg/μl *EN-SpTCF* in some cases formed a blastopore but did not complete gastrulation, and formed very few mesenchyme cells (Fig. 2I, O). The mesenchyme cells that form do not organize into the regular lattice structures of wild-type embryos (Fig. 2O).

Activated *TCF* (*VP16xTCF3*) vegetalizes embryos. The embryos do not elongate at gastrulation, retaining a rounded appearance. The embryos form a broadly flattened region in the vegetal pole, indicative of an enlarged vegetal plate (Fig. 2D, J). Embryos injected with *VP16xTCF3* mRNA form a fused ciliary band (a complete band), an effect often seen in low dose ($\leq$10 mM) LiCl-treated embryos (not shown). Pigment cells are not significantly increased over control embryos (Table 1). However, the range of pigment cell number counted is greater than control embryos. Sectioning of injected embryos reveals a larger number of mesenchymal cells present in the blastocoel than in control embryos (Fig. 2P). These embryos generally do not form vestibules or rudiments at injection doses of 1.6 μg/μl or greater. The vegetal-plate-derived tissues of these embryos are generally disorganized. At a lower dose of *VP16xTCF3* (around 1.2 μg/μl) a partial rudiment forms in most embryos.

Table 1 *Heliocidaris erythrogramma* eggs were injected with either 0.8 μg/μl *EN-SpTCF*, 1.6 μg/μl *VP16xTCF3*, or a control RNA, and then fertilized. Eggs were also fertilized and then incubated in 20 mM LiCl. At 43 h of development pigment cells were counted under a dissecting microscope. Statistically significant values are highlighted in *bold*

Pigment cells	Control injected	20 mM LiCl	*EN-SpTCF*	*VP16xTCF3*
Mean	195.6	299.8	1.3	194.5
SD	15.33	15.8	2.5	25.4
Count	11	5	11	10
Significance		**0.0004**	**0.0001**	0.78

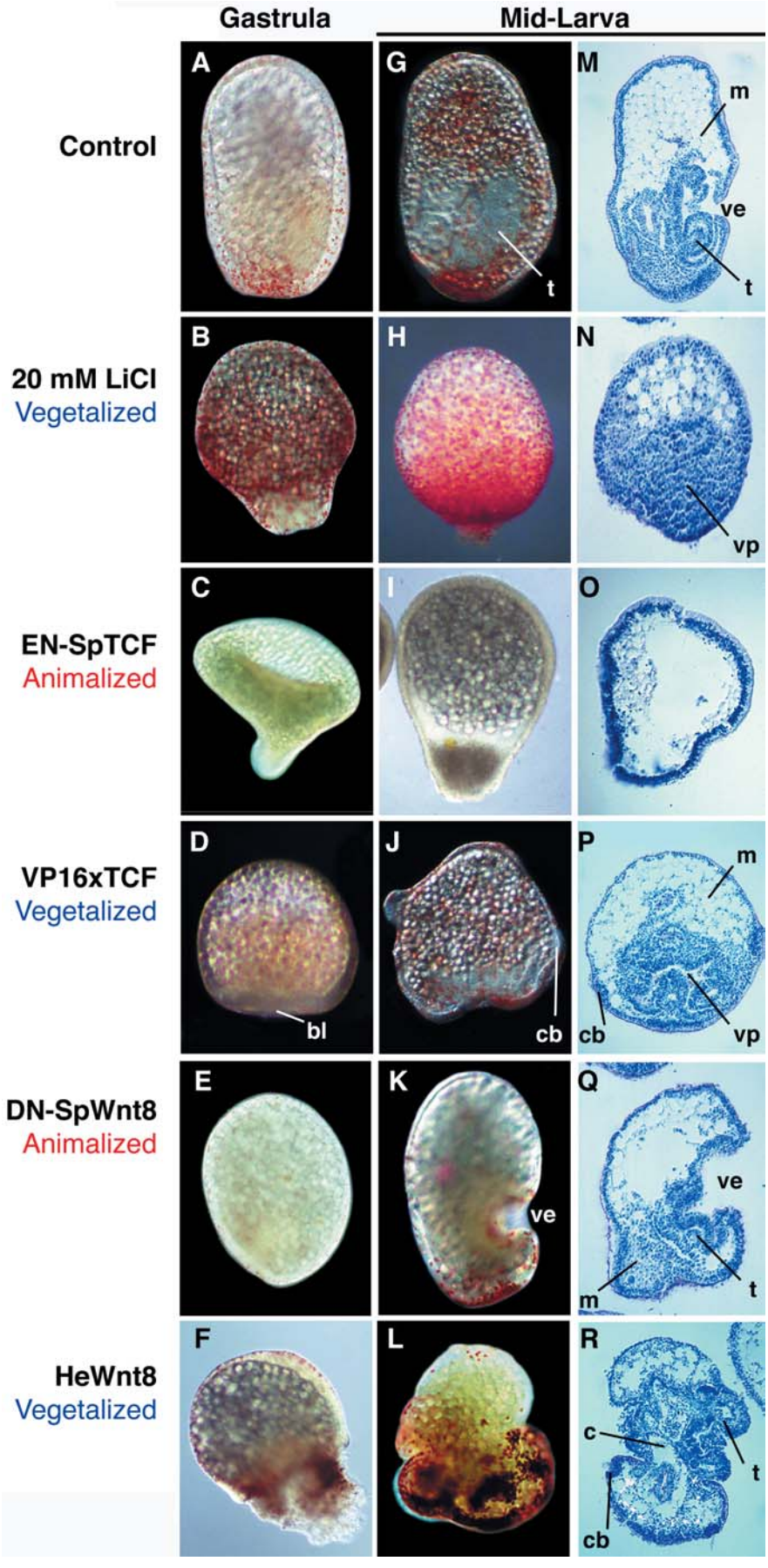

Fig. 2A–R The canonical Wnt pathway functions to pattern the vegetal pole of the *Heliocidaris erythrogramma* embryo. **A–F** Light micrographs of live, gastrula-stage *H. erythrogramma* embryos. **G–L** Live, mid-larva-stage *H. erythrogramma* embryos. **M–R** Embryos from **G–L** were sectioned and a representative medial section is shown which transverses the A/V axis of the mid-larva-stage embryo. Tissue sections were stained with toludine blue and eosin to label nuclei and cytoplasm respectively. **A**, **G**, **M** Images of control injected *H. erythrogramma* embryos. A rudiment is visible in **G** and **M**. Five regular tube feet are present (two are visible in the section in **M**). Embryos in **B**, **H** and **N** were treated with 20 mM LiCl from the 2-cell stage through gastrulation. These embryos are vegetalized. **C**, **I**, **O** Embryos were injected with *EN-SpTCF*. These embryos show a strongly animalized phenotype. **D**, **J**, **P** Images of *VP16xTCF*-injected embryos. Embryos in **D**, **J** and **P** exhibit a vegetalized phenotype, though not as severe as that seen in Li-treated embryos. **E**, **K**, **Q** Embryos injected with a *DN-Sp-Wnt8* construct. These embryos are partially animalized. **F**, **L**, **R** Images of *HeWnt8*-injected embryos. *HeWnt8*-injected embryos exhibit a partially vegetalized phenotype. Embryos are oriented where possible with the animal pole *up*, vegetal *down*, and larval left to the viewers *right*. (*C* coelomic tissue, *M* mesenchyme, *T* tube-foot, *Bl* blastopore, *Ve* vestibule, *Cb* ciliary band, *Hy* hydrocoel, *Vp* vegetal-plate-derived tissues)

Wnt8 and the role of a Wnt ligand in vegetal axis patterning

Embryos injected with *DN-SpWnt8* are animalized and exhibit a conversion of mesendoderm to ectoderm, but form normal ectoderm. Outwardly larval stage embryos appear to develop normally and show no sign of developmental abnormality aside from an enlarged vestibule (Fig. 2K, Q). Sectioning shows that *DN-SpWnt8*-injected embryos form a vestibule and pre-podial extensions of the vestibular ectoderm. However, coelomic and endodermal tissues are reduced and do not form a complete rudiment. In most instances fewer than half of the "tubefeet" which form in the vestibule contain internal mesodermal elements (Fig. 2Q). The number of pigment cells observed in *DN-SpWnt8*-injected embryos appears lower than in controls.

Misexpression of *HeWnt8* mRNA vegetalizes the embryo via conversion of ectoderm to mesendoderm. Injection of high doses of *HeWnt8* mRNA (1.4 μg/μl) into *H. erythrogramma* embryos results in the proliferation of mesenchyme cells that dissociate from the embryo during gastrulation (Fig. 2F). Sections of a mid-gastrula-stage *HeWnt8*-injected embryo (not shown) reveal the disintegration of the epithelium derived from the vegetal plate, and an enlarged vegetal tissue field, marked by a enlarged blastopore and archenteron, as gastrulation proceeds. At lower doses (1 μg/μl) *HeWnt8*-injected embryos fail to elongate. There is a thickening of the ectoderm on the left side, which is indicative of formation of presumptive vestibular ectoderm (Fig. 2F). Following gastrulation the developing larva maintains an animal-vegetal polarity. Around the mid-larva stage (>40 h), *HeWnt8*-injected embryos form ectodermal projections along the midline and animal pole region that resemble ectopic tubefeet (Fig. 2L, R). Internally, mid-larva-stage *HeWnt8*-injected embryos exhibit increased formation of coelomic cavities and other mesodermal structures. Skeletal elements form near the pigmented (vegetal) end of the embryos.

HeWnt8 mRNA expression is independent of *TCF* function in *H. erythrogramma*

In both indirect-developing species and *H. erythrogramma TCF* mRNA is expressed both as a maternal and zygotic message. In the indirect-developing sea urchin *S. purpuratus*, *Wnt8* mRNA expression is first detectable at the 16-cell stage (Angerer and Angerer 2000; Brandhorst and Klein 2002), and zygotic expression of *SpWnt8* mRNA is dependant on proper function of the canonical Wnt pathway (Wikramanayake, personal communication; Davidson et al. 2002). Expression of *HeWnt8* was assayed by RT-PCR (Fig. 3A). RT-PCR indicates that in *H. erythrogramma*, *HeWnt8* mRNA expression is first detectable at the 128-cell stage (Fig. 3A). There is therefore a three-cleavage cycle delay in timing of onset of *HeWnt8* expression as compared to that reported for *S. purpuratus*. In *H. erythrogramma* there is a 2-h delay

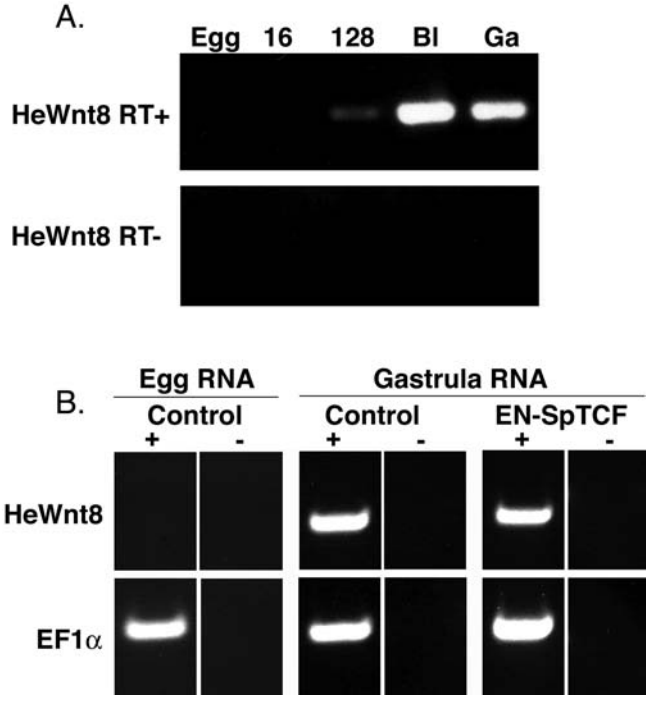

Fig. 3 Expression of HeWnt8 RNA is not dependant on TCF function. **A** RT-PCR was performed on total RNA collected from unfertilized eggs (Egg); 16-cell stage (16); 128-cell stage (128); hatched blastula (Bl); and mid-gastrula (Ga). PCR reactions in the absence of reverse transcriptase (RT-) did not show amplification of the target sequence. **B** RT-PCR was preformed using RNA isolated from control injected or *EN-SpTCF*-injected zygotes at the gastrula stage. Primers made to *HeWnt8* and *Ef1α* were used to assay *HeWnt8* expression and *EF1α* was used as a positive control. Reverse transcription reactions are indicated with a (+), control reactions without a reverse transcription step are indicated with a (–). Amplification is only observed in lanes in which a RT reaction was performed. *Wnt8* is present at significant levels in both control and *EN-SpTCF*-injected embryos

(four cleavage cycles) between the timing of β-catenin nuclear localization at the 8-cell stage (data not shown) and onset of *HeWnt8* expression at the 128-cell stage. We asked if *HeWnt8* is a downstream target of *TCF* transcriptional activation in *H. erythrogramma*.

H. erythrogramma eggs were injected with an *EN-SpTCF* transcript (0.6 μg/μl) or control RNA. Eggs were fertilized and embryos reared to the gastrula stage. Total RNA was extracted from 20 embryos in each treatment group. RT-PCR was preformed on control and *EN-SpTCF*-injected embryo RNAs (Fig. 3B). Primers HeW85 and HeW83, or EF15 and Ef13 were used to amplify *HeWnt8* or as a control, *EF1α*. Uninjected egg RNA was also isolated and subjected to RT-PCR. An *EF1α* signal is present in egg total RNA and *HeWnt8* is not (Fig. 3B). An *HeWnt8* PCR product is present in gastrula-stage RNA samples from both control and *EN-SpTCF*-injected embryos. These data suggest that *HeWnt8* expression is not regulated by *TCF* in *H. erythrogramma*.

TCF is functionally epistatic to *HeWnt8* in *H. erythrogramma*

The timing of *HeWnt8* expression has been shifted later in development compared to indirect-developing sea urchins and misexpression produces a vegetalization phenotype in *H. erythrogramma* embryos (Fig. 2F, L, R). Due to the changes in timing of expression and independence for maintenance of mRNA expression by *TCF* we generated two hypotheses. In the first, *Wnt8* is acting through the canonical Wnt pathway, and thus via *TCF*. Therefore any *TCF* phenotype will be epistatic to *HeWnt8*. Alternatively, *HeWnt8* acts though another signaling system such as the PCP pathway, as has been proposed by others (Wikramanayake, personal communication). Thus, when *HeWnt8* is co-injected with *EN-SpTCF* we should observe a partial rescue of the *EN-SpTCF*-induced animalization phenotype.

EN-SpTCF was injected at a concentration identical to that which was used to generate an animalized phenotype (0.6 μg/μl), and *HeWnt8* was co-injected at a level that would normally produce an *HeWnt8* misexpression phenotype (1 μg/μl), and was also co-injected at a higher dosage (1.4 μg/μl). Co-injected embryos showed the same phenotype seen in embryos injected with *EN-SpTCF* alone (not shown). Embryos lacked pigmentation and showed highly reduced endoderm, mesoderm, and mesenchyme at the gastrula and late larva stages. The *EN-SpTCF*:*HeWnt8*-co-injected embryos phenocopied *EN-SpTCF*-injected embryos. Embryos exhibited a lack of pigment cells, failed to form mesoderm or endoderm, and appeared animalized. However, co-injected embryos did form PMCs.

Tissue-specific markers in *H. erythrogramma* development

Patterns of tissue-specific markers in control embryos are references for analyzing changes in tissue specification following perturbation. Arylsulfatase (*HeARS*) is expressed throughout the ectoderm of the *H. erythrogramma* embryo at the mesenchyme blastula. *HeARS* expression resolves by the mid-larval stage to vestibular ectoderm and cells in the ciliary band (Haag and Raff 1998; Fig. 4G). Alkaline phosphatase is expressed in the gut, hydrocoel, and a subset of secondary mesenchyme cells in larval stage tissues (Fig. 4M). MSP130 is expressed in the skeletogenic primary mesenchyme cells (Anstrom et al. 1987; Klueg et al. 1997). At larval stages MSP130 is expressed in PMCs, which are localized in the vegetal third of the embryo (Fig. 4S).

The effects of vegetalization by lithium

HeARS expression is not detectable in embryos which were vegetalized with Li treatment (Fig. 4H). Embryos treated with 20 mM LiCl exhibit alkaline phosphatase staining (blue) throughout the embryo (Fig. 4N), indicating that all tissues including the presumptive ectoderm express some level of active alkaline phosphatase enzyme, normally only expressed in cells derived from the vegetal plate. MSP130-positive cells are located in the vegetal end of the embryos arrayed along the blastocoel wall (Fig. 4T). MSP130 expression is moderately lower than that of control embryos. The effects of Wnt pathway perturbation are summarized in Fig. 5.

The role of *TCF* in *H. erythrogramma* development

Embryos injected with *EN-SpTCF* mRNA express *HeARS* ubiquitously in the ectoderm at mid-larva stages (Fig. 4I). The ectoderm fails to differentiate vestibular ectoderm or a ciliary band. Alkaline phosphatase is not expressed in these animalized embryos (Fig. 4O). MSP130 antibody staining reveals that the few mesenchyme cells observed in the blastocoelar spaces of *EN-SpTCF*-injected embryos are positive for MSP130 (Fig. 4U), and therefore are primary mesenchyme cell derivatives.

Expression of *HeARS* was assayed in *VP16xTCF3*-injected embryos by whole-mount in situ hybridization. *HeARS* is expressed at low levels in a ring of ectoderm that is adjacent to the ciliary band, near the midline of the embryo (Fig. 4J). These embryos did not form vestibules or rudiments at injection doses of 1.4 μg/μl or greater. Staining for endogenous alkaline phosphatase activity indicates only faint and localized areas of alkaline phosphatase expression in blastocoelar cells (Fig. 4P). An antibody to MSP130 was used to assay if the internal cells were primary mesenchyme rather than secondary mesenchyme. Elevated levels of MSP130 staining are seen in *VP16xTCF3*-injected embryos (Fig. 4V) as compared to controls or LiCl-treated embryos. MSP130-positive cells are observed along the interior of the blastocoel wall throughout the embryo rather than in the vegetal locations observed in control and Li-treated embryos. MSP130-positive cells normally contribute to the formation of the larval skeleton. *VP16xTCF3*-injected embryos did not form skeletal elements up to as late as 60 h of development. The localization of MSP130-positive cells to the animal pole of the embryo indicate that the vegetal domain has extended upwards toward the animal pole converting ectodermal cells to vegetal fates. The fused ciliary band indicates that the larval dorsal/ventral and L/R axes have been partially disrupted in the *VP16xTCF3*-injected embryos. In spite of the apparent increase in MSP130-positive cells larval skeleton does not form. Thus, the PMCs fail to adopt a completely differentiated, functional skeletogenic cell fate.

Wnt8 and the role of a Wnt ligand in patterning

The expression of *HeARS* is localized to the vestibular ectoderm in embryos injected with *DN-SpWnt8* (Fig. 4K) as in controls. Endogenous alkaline phosphatase activity

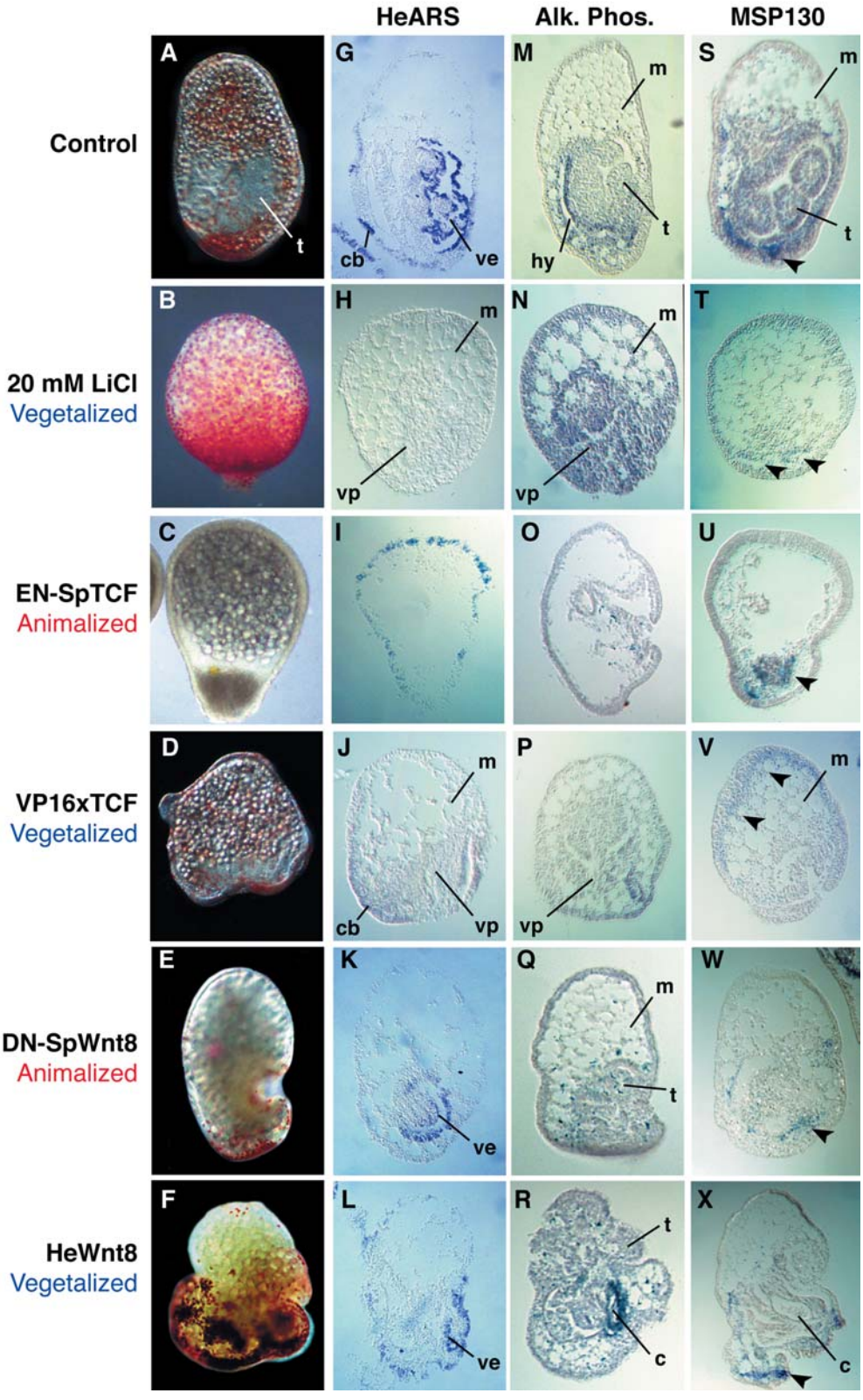

Fig. 4 Tissue specific effects of Lithium, TCF, and Wnt8 on H. erythrogramma. The rows of embryos are as follows, **A**, **G**, **M**, and **S** are control injected embryos. **B**, **H**, **N**, and **T** are 20 mM LiCl treated. **C**, **I**, **O**, and **U** *EN-SpTCF*-injected. **D**, **J**, **P**, and **V**, *VP16xTCF3*-injected. **E**, **K**, **Q** **W**, *DN-SpWnt8*-injected embryos, and **F**, **L**, **R**, and **X** are *HeWnt8*-injected. In the columns, **A–F** are light micrographs of live larval stage embryos. **G–L** are WISH with a *HeARS* antisense riboprobe in larval stage embryos. **M–R**, endogenous alkaline phosphatase stained embryos, and **S–X** are sections of embryos stained for MSP130. In **S–X** arrows indicate areas of MSP130 positive cells. For all panels, embryos are oriented where possible with the animal pole up, vegetal down, and larval left to the viewers right., c coelomic tissue, m mesenchyme, t tubefoot, ve vestibule, vp vegetal plate derived tissue, hy hydrocoel

in the *DN-SpWnt8* embryos is present in mesenchyme cells in the blastocoel and weakly in a cluster of cells that may be coelomic tissue remnants (Fig. 4Q). Staining for MSP130 indicates that primary mesenchyme cells are present. They localize to the vegetal pole and are present in approximately equal numbers to control embryos.

Whole-mount in situ hybridization with *HeARS* in *HeWnt8*-injected embryos indicates that vestibular ecto-

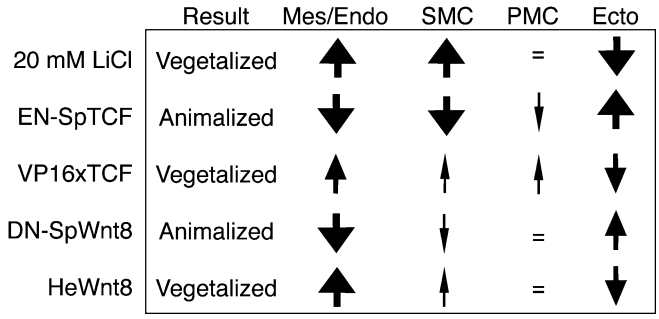

Fig. 5 Summary of the effects of Wnt pathway molecules studied in this paper on *H. erythrogramma*. *Arrows pointing up* indicate an increase in, or conversion to the given tissue type. *Arrows pointing down* indicate a decrease in the amount of a tissue type. The thickness of the arrows indicate the relative degree of tissue increase or decrease compared to controls. *Mesendo* mesendodermal tissues, gut, and coelomic tissues, SMC secondary mesenchyme cells, PMC primary mesenchyme cells, Ecto ectoderm

derm differentiates and forms on one side of the embryo consistent with left-right axis patterning (Fig. 4L). Endogenous alkaline phosphatase localization in embryos injected with *HeWnt8* indicates that a larger than normal number of cells express alkaline phosphatase. A light blue signal is observable in many tissues and an increase in the number of SMCs positive for alkaline phsophatase compared with control embryos is also visible (Fig. 4R). Dark blue staining is evident in an enlarged hydrocoel, which indicates that coelomic tissues do partially differentiate, more so than seen in LiCl-treated embryos. Antibody staining for MSP130 indicates that the localization and number of PMC cells in *HeWnt8*-injected embryos is the same as control embryos.

The effect of LiCl on development on another direct-developing sea urchin species, *Holopneustes purpurescens*

H. purpurescens is an independently evolved direct-developing sea urchin separated from *H. erythrogramma* by approximately 70 million years (Smith 1988). *H. purpurescens* belongs to the family Temnopleuridae (Fig. 6I), which includes a clade of sea urchins that evolved a lecithotropic, direct-developmental mode 4–7 million years ago (Jeffery et al. 2003). Therefore we tested the functional roles of *Wnt8* and *TCF* in *H. purpurescens* to determine if the role of the Wnt pathway in vegetal axis specification is conserved among the major euechinoid clades and in an independently evolved direct-developer.

H. purpurescens zygotes were treated with 20 mM LiCl through 24 h of development, then removed from LiCl and transferred to MPFSW and cultured to larval stages. LiCl-treated embryos failed to elongate and retained an unclosed blastopore (Figure 6B). The blastopore of control-injected *H. purpurescens* embryos closes after gastrulation. As in *H. erythrogramma*, LiCl treatment induces an increased mesenchyme cell production, which was quantified by counting pigment cells on the embryos at 45 h of development (Table 2). LiCl treatment resulted in a significant increase in pigment cells over control embryos. An increased number of mesenchyme cells was observed in the blastocoel of embryos (Fig. 6F). A mass of vegetal-plate-derived tissue occupies the center of the blastocoel.

TCF constructs reveal a conserved role for the Wnt pathway in patterning the A/V axis of *Holopneustes purpurescens*

EN-SpTCF mRNA animalizes *H. purpurescens*. *EN-SpTCF* mRNA injection results in a blastula-like embryo, which forms multiple hollow lobes. In some cases (Fig. 6C, G) a highly reduced and mostly undifferentiated rudiment primordium will form in part of one lobe. This is the result of incomplete blockage of all vegetal fates at low doses of *EN-SpTCF*. Consistent with an animalization phenotype, pigment cell numbers are highly reduced or absent in injected embryos (Table 2). Mesenchyme cells are reduced in number within the blastocoel (Fig. 6G). These phenotypes are also consistent with those seen in *H. erythrogramma*.

Embryos injected with *VP16xTCF3* failed to elongate, similar to LiCl-treated embryos (Fig. 6D). The blastopore opening was generally larger than that seen in LiCl-treated embryos and also failed to close. Internal mesenchyme cell numbers were approximately the same as those seen in wild-type embryos. Pigment cell counts are also not statistically different from control embryos (Table 2). A partial rudiment does form in these embryos, at the vegetal end of the embryo inside the opened blastopore (Fig. 6H). Wild-type embryos form five primary podia. However, *VP16xTCF3*-injected embryos formed no more than four primary podia and generally only two or three. These embryos fail to organize a

Table 2 *Holopneustes purpurescens* eggs were injected with either 0.8 μg/μl *EN-SpTCF*, 1.6 μg/μl *VP16xTCF3*, or a control RNA, and then fertilized. Eggs were also fertilized and then incubated in 20 mM LiCl. At 43 h of development pigment cells were counted under a dissecting microscope. Statistically significant values are highlighted in *bold*

Pigment cells	Controls injected	20 mM LiCl	*EN-SpTCF*	*VP16xTCF3*
Mean	97	143	11.6	109.5
SD	16.7	20.5	12.6	29.24
Count	11	11	11	11
Significance		**<0.0001**	**<0.0001**	0.28

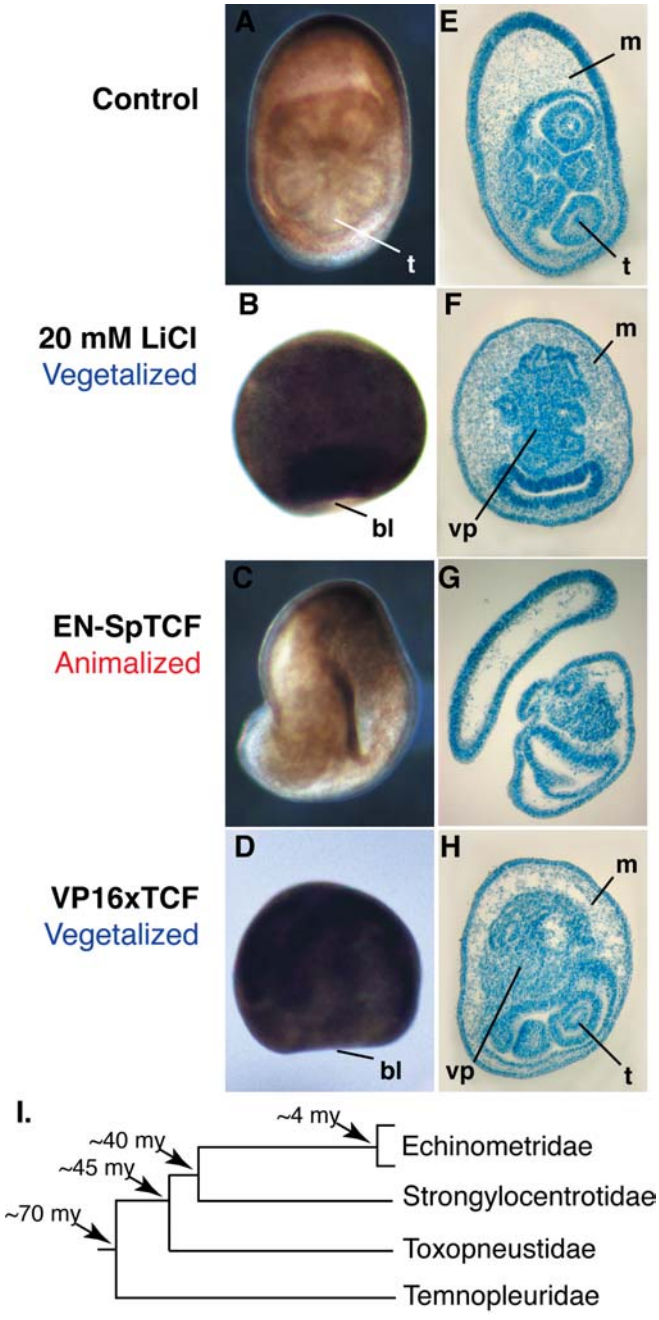

Fig. 6 The activity of Wnt signaling pathway molecules in *H. purpurescens*. **A–D** *H. purpurescens* embryos imaged live at 42–46 hours of development (mid-larva stage). **E–H** *H. purpurescens* embryos 9 um sections, where possible embryos are oriented with larval left to the viewer's right. For all embryos animal pole is up and vegetal down. **A** and **E** 44-h *H. purpurescens* embryos which were injected with buffer. A normal pentameral rudiment is visible in both panels. **B** and **F** 25 mM LiCl treated *H. purpurescens* embryos. Note the enlarged, unclosed blastopore and the rounded appearance of the embryo. **F** shows an increase in mesenchyme cells in the blastocoel, a well formed archenteral cavity at the vegetal end, and a large, mass of vegetal plate dervied tissues above. **C** and **G**; 44 hour embryos injected with *EN-SpTCF*. The embryos form multiple protruding lobes. The section in **G** shows two lobes of the embryo. Panels **D** and **H**; *VP16xTCF3*-injected embryos. Note the large, open blastopore in panel **D**. In **H** three tube feet are visible. A large mass of endoderm and coelomic mesoderm are visible in the center of the embryo as in **G**. For all embryos; T tubefoot, Bl blastopore, M mesenchyme, Vp vegetal plate derived tissue. **I** A phylogeny of sea urchin taxa. Phylogeny based on the taxonomic work of Smith (1988) and Jeffery et al. (2003). The Temnopleuridae (*Holopneustes purpurescens*) are approximately 70 million years diverged from the Echinometridae (*Heliocidaris erythrogramma* and *Heliocidaris tuberculata*). The Strongylocentrotidae (*Strongylocentrotus purpuratus*) and Toxopneustidae (*Lytechinus variegatus*) are approximately 40 million years diverged from *H. erythrogramma*. In this paper we present data from *H. erythrogramma*, and *H. purpurescens*, two independently derived direct-developing sea urchins, on the function of the canonical Wnt pathway in axis patterning

rudiment that is competent to metamorphose. These effects are consistent with the effects of *VP16xTCF3* mRNA in *H. erythrogramma*.

Discussion

Conservation of Wnt pathway function

In this study we show that the role of the canonical Wnt pathway in specification of the vegetal pole of the sea urchin embryo is conserved in euechinoid taxa, and most importantly in the highly modified ontogenies of direct-developing urchins. We demonstrate that there is a conserved functional role for *Wnt8* in patterning the endomesoderm, and that *TCF* is necessary for early specification of vegetal tissues and, in part, patterning the ectodermal territories. These observations are consistent with those of studies of indirect-developing species (Emily-Fenouil et al. 1998; Huang et al. 2000; Vonica et al. 2000). We also demonstrate several divergences between *Heliocidaris erythrogramma* and indirect-developing sea urchins Wnt pathway components. First, in *H. erythrogramma* the initial timing of *Wnt8* expression begins three cleavage cycles later than that seen in indirect-developing species (Fig. 3A). Second, the maintenance of expression of *HeWnt8* is not dependant on proper *TCF* function. Third, in *H. erythrogramma TCF* may not be involved in specifying the PMCs, or is to a lesser degree, as compared with indirect-developing sea urchins. The observed differences are correlated with the transition from indirect- to direct-developing early ontogenies.

The degree to which Wnt signaling is conserved in patterning the A/V axis of the direct-developing sea urchin *H. erythrogramma*, a sea urchin with such a modified developmental program, is significant. Despite rapid evolution of timing and specification of the other embryonic axes, the Wnt pathway components *Wnt8* and *TCF* are largely conserved in their functions. This implies a strong requirement for or possibly underlying developmental constraint to retain the canonical Wnt pathway in vegetal axis specification.

Activated *TCF* vegetalizes embryos and dominant negative *TCF* has a reciprocal animalizing effect (Fig. 5), consistent with the functional role of *TCF* seen in similar experiments in *S. purpuratus* (Huang et al. 2000; Vonica

et al. 2000). LiCl strongly vegetalizes treated *Heliocidaris erythrogramma* and *Holopneustes purpurescens* embryos. This phenotype is consistent with the effects seen in indirect-developing urchins and implicates the Wnt signaling pathway in patterning the vegetal end of the A/V axis of echinoids. The role of the ligand *HeWnt8* in the development of *H. erythrogramma* lies in mesendoderm specification. This role is similar to that reported for *Wnt8* in indirect-developing sea urchins (Angerer and Angerer 2000; Brandhorst and Klein 2002). Our data confirms that the canonical Wnt pathway, signaling through *TCF*, is directly involved in patterning the vegetal axis of the *H. erythrogramma* embryo. Even among highly divergent early developmental ontogenies the general functional outputs of the Wnt pathway are conserved in defining and patterning the A/V axis of sea urchin embryos.

The effects of the *VP16xTCF3* are not fully congruent with changes seen in *H. erythrogramma* embryos treated with LiCl. LiCl is known to affect several different signaling pathways besides the Wnt pathway, including Hedgehog (Jia et al. 2002), PI (Forer and Sillers 1987), and ion channel function (Hermoni et al. 1987). Because lithium effects other signaling pathways the observed differences between *VP16xTCF3* and LiCl treatment could lie with perturbations of these pathways as well. None the less, the vegetalizing effects of lithium are generally consistent among sea urchins.

The direct-developing sea urchins *H. erythrogramma* (Williams and Anderson 1975) and *H. purpurescens* (Morris 1995) do not exhibit unequal cleavages in development. Micromeres are not formed during cleavage. Thus, the role of the Wnt pathway in initial signaling in the micromeres is not inextricably tied to an unequal cleavage event. However, *β-catenin* is required for the PMC cell fate specification in indirect-developing sea urchins.

Divergence of Wnt pathway components in a direct-developing ontogeny

The Wnt pathway molecules examined here, *TCF*, *β-catenin* (via lithium treatment) and *Wnt8*, appear to function in a manner similar to that seen in indirect-developing sea urchins. However, the temporal profile of activity of these molecules has changed. In indirect-developers, β-catenin protein nuclear localization is first detected in the micromeres at the 16-cell stage, and then several cleavages later can be seen in the nuclei of most vegetal blastomeres (Logan et al. 1999). This indicates that, in indirect developers, *TCF* contributes to sequential specification of a PMC field first and then progressively incorporates more tissue into the vegetal field. In *Heliocidaris erythrogramma TCF* functions to specify a vegetal morphogenetic field. The data presented from *H. erythrogramma* indicate that PMC specification occurs later in development than seen in indirect-developing sea urchin embryos. This is consistent with fate mapping studies, which show that PMCs are not determined until the 128-cell stage or later in *H. erythrogramma* (Wray and Raff 1990).

We identify a possible change in the mechanism of PMC specification. Among indirect-developing sea urchins, the *SpAlx1* and *pmar1* genes are involved in the early determination of PMC cell fates specification and both are upstream of MSP130 expression (Oliveri et al. 2002; Ettensohn et al. 2003). The expression of *SpAlx1* and *pmar1* genes are thought to be initially regulated by and dependent upon maternal *β-catenin/TCF* signaling (Davidson et al. 2002). Inhibition of canonical Wnt signaling via misexpression of *E-cadherin* or *DN-TCF* injection reduces PMCs (Huang et al. 2000; Vonica et al. 2000; Ettensohn et al. 2003).

EN-SpTCF can animalize without inhibiting PMC specification, and *VP16xTCF3* can induce vegetalization without significantly increasing mesenchyme cells in both *H. erythrogramma* and *Holopneustes purpurescens*. *EN-SpTCF* appears to inhibit specification of all vegetal structures except PMCs. This is not consistent with observations of *EN-SpTCF* in *S. purpuratus* or *Lytechinus variegatus*, where vegetal tissues, including PMCs, are not formed (J. Venuti, personal communication). Thus, the role of *TCF* in specification of all vegetal structures in *H. erythrogramma* and *H. purpurescens* appears to be somewhat different to that observed in indirect-developing urchins but is consistent with previous morphological observations (Wray and Raff 1990).

The specification of the primary mesenchyme cells in *H. erythrogramma* is not completely dependant on *TCF* function, and this is divergent from what is observed in indirect-developing urchins (Huang et al. 2000). Lithium treatment, however, does not result in an increase in all vegetal cell types. MSP130 staining indicates that there is no significant increase in the number of PMCs or a change in their localization within the embryo following lithium treatment. Even at high doses of *EN-SpTCF* mRNA, (0.9 or 0.8 μg/μl) formation of PMCs was not inhibited in *H. erythrogramma*. This incomplete inhibition is distinct from the results reported for DN-TCF-injected into *S. purpuratus,* and *L. variegatus*. In *S. purpuratus*, PMC formation was inhibited in greater than 90% of injected embryos (Huang et al. 2000) and a similar phenotype was observed with *EN-SpTCF* injected into *S. purpuratus* and *L. variegatus* embryos (J. Venuti, personal communication). This same phenotype, a loss of PMCs, is observed in two families of indirect-developing sea urchins, 40 my diverged (Fig. 6I). However, a different phenotype, retention of PMCs following *EN-SpTCF* injection, is observed in *H. erythrogramma*. These findings are suggestive of a functional change in the role of *TCF*. From this evidence we conclude that in both indirect- and direct-developing sea urchin species, *TCF* is necessary as a part of the early determination and specification of a vegetal field. However, these data further indicate a possible novel variation of *TCF* signaling in *H. erythrogramma*, an uncoupling or weak-

ening of the linkage between specification of PMCs and the activity of *TCF* in the early embryo.

Injection of the *EN-SpTCF* construct failed to reduce the endogenous levels of *HeWnt8* RNA in gastrula-stage *H. erythrogramma* embryos, showing that in *H. erythrogramma* maintenance of *HeWnt8* expression is not driven by *TCF*. However, the phenotypic effects of *TCF* expression are epistatic to *HeWnt8*. This result would be expected if *Wnt8* signaled through *TCF*, or if *TCF* is required for inducing competence of vegetal tissues to respond to other vegetalizing gene products including *HeWnt8*.

Phylogenetic comparisons of Wnt signaling in divergent life histories

Injection of activated and dominant negative *TCF* as well as LiCl treatment have similar effects on both *Heliocidaris erythrogramma* and *Holopneustes purpurescens*. The phenotypes are similar to those seen in indirect-developing sea urchins (Wikramanayake and Klein 1997; Wikramanayake et al. 1998; Logan et al. 1999; Vonica et al. 2000). This similarity indicates a strong functional conservation of the Wnt pathway in formation and patterning of the A/V axis among echinoids. Despite distinct changes in composition of the eggs (Villinski et al. 2002), cleavage pattern (Henry et al. 1990), number of cleavages prior to gastrulation (Parks et al. 1988), cell fates and patterning (Wray and Raff 1990), *H. erythrogramma* uses the Wnt pathway and the gene *HeWnt8* functionally, in a similar manner to *S. purpuratus*. Through about 70 million years of evolution, *H. erythrogramma* and *H. purpurescens* independently evolved convergent life histories (Raff et al. 2003), but the Wnt signaling system has remained remarkably stable in functional output between the two species.

Conclusions

We have shown that the role of the Wnt pathway in vegetal axis specification is conserved in highly divergent sea urchin ontogenies. Such conservation of the canonical Wnt pathway for specification of the vegetal field of *Heliocidaris erythrogramma*, in light of significant changes in timing of axial specification and patterning, suggest a conserved constraint on Wnt involvement in A/V axis patterning among deuterostomes. *TCF* and *β-catenin* specify a vegetal morphogenetic field, and *Wnt8* plays a role in specification of coelomic, mesendodermal tissues. We also show that, even within this overall conservation, divergence may be evolving in the roles of these component genes.

Acknowledgements This work was supported by an NSF grant to R.A.R. and a NSF IGERT fellowship to J.S.K. We thank the School of Biological Science, University of Sydney, NSW, and the Sydney Aquarium for generously providing facilities. We thank B. Sly and J. Kumar for critical reading of the manuscript, M. Andrews for technical assistance, and V. Morris for discussions and assistance with *Holopneustes*. We also thank J. Venuti and A. Wikramanayake for expression constructs.

References

Angerer LM, Angerer RC (2000) Animal-vegetal axis patterning mechanisms in the early sea urchin embryo. Dev Biol 218(1):1–12

Angerer LM, Angerer RC (2003) Patterning the sea urchin embryo: gene regulatory networks, signaling pathways, and cellular interactions. Curr Top Dev Biol 53:159–198

Anstrom JA, Chin JE, Leaf DS, Parks AL, Raff RA (1987) Localization and expression of *msp130*, a primary mesenchyme lineage-specific cell surface protein in the sea urchin embryo. Development 101(2):255–265

Brandhorst BP, Klein WH (2002) Molecular patterning along the sea urchin animal-vegetal axis. Int Rev Cytol 213:183–232

Byrne M, Villinski JT, Cisternas P, Siegel RK, Popodi E, Raff RA (1999) Maternal factors and the evolution of developmental mode: evolution of oogenesis in *Heliocidaris erythrogramma*. Dev Genes Evol 209:275–283

Cadigan KM, Nusse R (1997) *Wnt* signaling: a common theme in animal development. Genes Dev 11(24):3286–3305

Cameron RA, Davidson EH (1997) LiCl perturbs ectodermal veg1 lineage allocations in *Strongylocentrotus purpuratus* embryos. Dev Biol 187(2):236–239

Cameron RA, Hough-Evans BR, Britten RJ, Davidson EH (1987) Lineage and fate of each blastomere of the eight-cell sea urchin embryo. Genes Dev 1(1):75–85

Davidson EH, Cameron RA, Ransick A (1998) Specification of cell fate in the sea urchin embryo: summary and some proposed mechanisms. Development 125(17):3269–3290

Davidson EH, Rast JP, Oliveri P, Ransick A, Calestani C, Yuh CH, Minokawa T, Amore G, Hinman V, Arenas-Mena C, Otim O, Brown CT, Livi CB, Lee PY, Revilla R, Schilstra MJ, Clarke PJ, Rust AG, Pan Z, Arnone MI, Rowen L, Cameron RA, McClay DR, Hood L, Bolouri H (2002) A provisional regulatory gene network for specification of endomesoderm in the sea urchin embryo. Dev Biol 246(1):162–190

Emily-Fenouil F, Ghiglione C, Lhomond G, Lepage T, Gache C (1998) *GSK3beta/shaggy* mediates patterning along the animal-vegetal axis of the sea urchin embryo. Development 125(13):2489–2498

Emlet RB, McEdward LR, Strathmann RR (1987) Echinoderm larval ecology viewed from the egg. In: Jangoux AAM, Lawrence JM (eds) Echinoderm studies 2. Balkema, Rotterdam, pp 55–136

Ettensohn CA, Illies MR, Oliveri P, De Jong DL (2003) *Alx1*, a member of the Cart1/Alx3/Alx4 subfamily of Paired-class homeodomain proteins, is an essential component of the gene network controlling skeletogenic fate specification in the sea urchin embryo. Development 130(13):2917–2928

Ferkowicz MJ, Stander MC, Raff RA (1998) Phylogenetic relationships and developmental expression of three sea urchin *Wnt* genes. Mol Biol Evol 15(7):809–819

Forer A, Sillers PJ (1987) The role of the phosphatidylinositol cycle in mitosis in sea urchin zygotes. Lithium inhibition is overcome by myo-inositol but not by other cyclitols or sugars. Exp Cell Res 170(1):42–55

Goldstein B, Freeman G (1997) Axis specification in animal development. Bioessays 19(2):105–116

Haag ES, Raff RA (1998) Isolation and characterization of three mRNAs enriched in embryos of the direct-developing sea urchin *Heliocidaris erythrogramma*: evolution of larval ectoderm. Dev Genes Evol 208(4):188–204

Henry JJ, Raff RA (1990) Evolutionary change in the process of dorsoventral axis determination in the direct-developing sea urchin, *Heliocidaris erythrogramma*. Dev Biol 141(1):55–69

Henry JJ, Wray GA, Raff RA (1990) The dorsoventral axis is specified prior to first cleavage in the direct-developing sea urchin *Heliocidaris erythrogramma*. Development 110(3):875–884

Hermoni M, Barzilai A, Rahamimoff H (1987) Modulation of the Na+-Ca2+ antiport by its ionic environment: the effect of lithium. Isr J Med Sci 23:44–48

Huang L, Li X, El-Hodiri HM, Dayal S, Wikramanayake AH, Klein WH (2000) Involvement of *Tcf/Lef* in establishing cell types along the animal-vegetal axis of sea urchins. Dev Genes Evol 210(2):73–81

Jeffery CH, Emlet RB, Littlewood DT (2003) Phylogeny and evolution of developmental mode in temnopleurid echinoids. Mol Phylogenet Evol 28(1):99–118

Jia J, Amanai K, Wang G, Tang J, Wang B, Jiang J (2002) *Shaggy/GSK3* antagonizes *Hedgehog* signaling by regulating *Cubitus interruptus*. Nature 416(6880):548–552

Kauffman JS, Zinovyeva A, Yagi K, Makabe KW, Raff RA (2003) Neural expression of the Huntington's disease gene as a chordate evolutionary novelty. J Exp Zool 297B(1):57–64

Klueg KM, Harkey MA, Raff RA (1997) Mechanisms of evolutionary changes in timing, spatial expression, and mRNA processing in the *msp130* gene in a direct-developing sea urchin, *Heliocidaris erythrogramma*. Dev Biol 182(1):121–133

Logan CY, Miller JR, Ferkowicz MJ, McClay DR (1999) Nuclear *beta-catenin* is required to specify vegetal cell fates in the sea urchin embryo. Development 126(2):345–357

Morris VB (1995) Apluteal development of the sea urchin *Holopneustes purpurescens* Agassiz (Echinodermata: Echinoidea: Euechinoidea). Zool J Linn Soc 114:349–364

Okazaki K (1975) Normal development to metamorphosis. In: Czihak G (ed) The sea urchin embryo. Springer, Berlin Heidelberg New York, pp 177–232

Oliveri P, Davidson EH, McClay DR (2002) Activation of *pmar1* controls specification of micromeres in the sea urchin embryo. Dev Biol 258(1):32–43

Parks AL, Parr BA, Chin JE, Leaf DS, Raff RA (1988) Molecular analysis of heterochrony in the evolution of direct-development in sea urchins. J Evol Biol 1:27–44

Raff EC, Popodi EM, Sly BJ, Turner FR, Villinski JT, Raff RA (1999) A novel ontogenetic pathway in hybrid embryos between species with different modes of development. Development 126(9):1937–1945

Raff EC, Popodi EM, Kauffman JS, Sly BJ, Turner FR, Morris VB, Raff RA (2003) Regulatory punctuated equilibrium and convergence in the evolution of developmental pathways in direct-developing sea urchins. Evol Dev 5(5):478–493

Raff RA (1987) Constraint, flexibility, and phylogenetic history in the evolution of direct-development in sea urchins. Dev Biol 119(1):6–19

Raff RA (1996) The shape of life: genes, development and the evolution of animal form. University of Chicago Press, Chicago, Ill.

Ransick A, Davidson EH (1993) A complete second gut induced by transplanted micromeres in the sea urchin embryo. Science 259(5098):1134–1138

Ransick A, Davidson EH (1995) Micromeres are required for normal vegetal plate specification in sea urchin embryos. Development 121(10):3215–3222

Sharpe C, Lawrence N, Martinez-Arias A (2001) *Wnt* signalling: a theme with nuclear variations. Bioessays 23(4):311–318

Sly BJ, Hazel JC, Popodi EM, Raff RA (2002) Patterns of gene expression in the developing adult sea urchin central nervous system reveal multiple domains and deep-seated neural pentamery. Evol Dev 4(3):189–204

Smith AB (1988) Phylogenetic relationship, divergence times, and rates of molecular evolution for camarodont sea urchins. Mol Biol Evol 5(4):345–365

Takata H, Kominami T, Masui M (2002) Role of cell contact in the specification process of pigment founder cells in the sea urchin embryo. Zool Sci 19(3):299–307

Villinski JT, Villinski JC, Byrne M, Raff RA (2002) Convergent maternal provisioning and life-history evolution in echinoderms. Evolution 56(9):1764–1775

Vonica A, Weng W, Gumbiner BM, Venuti JM (2000) TCF is the nuclear effector of the *beta-catenin* signal that patterns the sea urchin animal-vegetal axis. Dev Biol 217(2):230–243

Wikramanayake AH, Klein WH (1997) Multiple signaling events specify ectoderm and pattern the oral-aboral axis in the sea urchin embryo. Development 124(1):13–20

Wikramanayake AH, Huang L, Klein WH (1998) *beta-Catenin* is essential for patterning the maternally specified animal-vegetal axis in the sea urchin embryo. Proc Natl Acad Sci USA 95(16):9343–9348

Williams DHC, Anderson DT (1975) The reproductive system, embryonic development, larval development, and metamorphosis of the sea urchin *Heliocidaris erythrogramma* (Val.) (Echinoidea: Echinometridae). Aust J Zool 23:371–403

Wray GA, Raff RA (1989) Evolutionary modification of cell lineage in the direct-developing sea urchin *Heliocidaris erythrogramma*. Dev Biol 132(2):458–470

Wray GA, Raff RA (1990) Novel origins of lineage founder cells in the direct-developing sea urchin *Heliocidaris erythrogramma*. Dev Biol 141(1):41–54

Zigler KS, Raff EC, Popodi E, Raff RA, Lessios HE (2003) Adaptive evolution of bindin in the genus *Heliocidaris* is correlated with the shift to direct-development. Evolution 57(10):2293–2302